Journal of Organometallic Chemistry 693 (2008) 3923–3931

Contents lists available at ScienceDirect

Journal of Organometallic Chemistry

journal homepage: www.elsevier.com/locate/jorganchem

Rhodium complexes of 1,3-diaryltriazenes: Usual coordination, N–H bond activation and, N–N and C–N bond cleavage

Chhandasi GuhaRoy [a], Ray J. Butcher [b], Samaresh Bhattacharya [a,*]

[a] Department of Chemistry, Inorganic Chemistry Section, Jadavpur University, Kolkata 700 032, India
[b] Department of Chemistry, Howard University, Washington, DC 20059, USA

ARTICLE INFO

Article history:
Received 12 August 2008
Received in revised form 3 October 2008
Accepted 7 October 2008
Available online 14 October 2008

Keywords:
1,3-Diaryltriazenes
Rhodium
N–H bond activation
N–N and C–N bond cleavage
η^1-Aryl complexes

ABSTRACT

Reaction of 1,3-diaryltriazenes (R–C_6H_4–N=N–(NH)–C_6H_4–R, R = OCH_3, CH_3, H, Cl, NO_2 at the *para* position) with $[Rh(PPh_3)_3Cl]$ in ethanol in the presence of a base (NEt_3) affords a family of yellow complexes (**1-R**) containing a PPh_3, two de-protonated triazenes coordinated as bidentate N,N-donors, and an aryl (C_6H_4–R) fragment coordinated in the η^1-fashion. A similar reaction in toluene yields a group of reddish-orange complexes (**2-R**) containing a PPh_3, two N,N-coordinated triazenes, and a chloride. Structures of the **1-CH_3** and **2-CH_3** complexes have been determined by X-ray crystallography. All the **1-R** and **2-R** complexes are diamagnetic, and show characteristic ^1H NMR signals and intense MLCT transitions in the visible region. The **1-R** and **2-R** complexes also fluoresce in the visible region under ambient condition while excited at around 400 nm. Cyclic voltammetry on these complexes shows a Rh(III)–Rh(IV) oxidation (within 0.76–1.68 vs. SCE), followed by an oxidation of the coordinated triazene ligand (except the R = NO_2 complexes). An irreversible reduction of the coordinated triazene is also observed for all the complexes below −0.96 V vs. SCE. In the **1-R** and **2-R** complexes potential of the Rh(III)–Rh(IV) oxidation correlates linearly with the electron-withdrawing nature of the *para*-substituent (R).

1. Introduction

Though the Wilkinson's catalyst, *viz.* $[Rh(PPh_3)_3Cl]$, is famous for its catalytic application in bringing about numerous interesting chemical transformations [1], we have found it to be a useful synthon for the preparation of mixed-ligand complexes of various types [2–13]. Besides its demonstrated ability to accommodate new ligands, it has also been found to mediate many interesting reactions, such as C–H and C–C bond activation of organic molecules [2,5,9,12], activation of molecular oxygen [13], and transformation of coordinated ligands [5,9,11]. These interesting observations have prompted us to further continue our exploration on reaction of the Wilkinson's catalyst with organic ligands, and the present study has originated from this exploration. Herein we have selected a group of 1,3-diaryltriazenes (**L**) to interact with the Wilkinson's catalyst. These ligands usually binds to a metal center, via dissociation of the acidic N–H proton, as monoanionic bidentate N,N-donor forming a four-membered chelate ring (**I**) [14–24]. The 1,3-diaryltriazenide anion is a 'short-bite' ligand, which has received continuous and sustained interest in the research field because of its ability to serve as a monodentate [15,25–27], a bidentate chelating [14–24], and also a bridging ligand [28–37]. The chemistry of the triazene ligands is further important because of their biological relevance [38–40]. Reaction of 1,3-diaryltriazenes (**L**) with $[Rh(PPh_3)_3Cl]$ has indeed afforded complexes containing η^2-bound triazenes (**I**), but depending on the nature of the reaction medium interesting N–N and C–N bond cleavage of the 1,3-diaryltriazenes also has taken place affording organorhodium complexes having η^1-bound aryl fragment. The present report deals with the chemistry of all these complexes with special reference to their formation, structure and spectral and electrochemical properties.

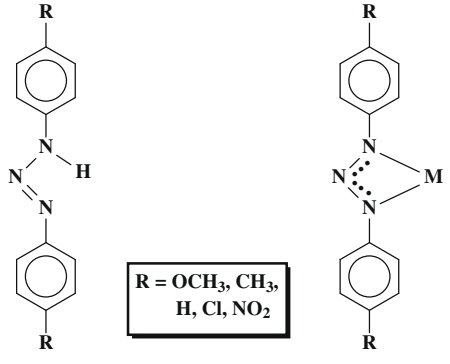

L I

* Corresponding author.
E-mail address: Samaresh_b@hotmail.com (S. Bhattacharya).

0022-328X/$ - see front matter © 2008 Elsevier B.V. All rights reserved.
doi:10.1016/j.jorganchem.2008.10.006

2. Results and discussion

2.1. Synthesis and characterization

As delineated in Section 1, the primary objective of the present study has been to see how 1,3-diaryltriazenes (**L**) react with the Wilkinson's catalyst, and a group of five 1,3-diaryltriazenes have been used in the present study, differing in the inductive effect of the *para*-substituents R, in order to observe their influence, if any, on the redox properties of the resulting complexes. Reactions of the 1,3-diaryltriazenes with $[Rh(PPh_3)_3Cl]$ has been carried out in refluxing ethanol in the presence of triethylamine [41], which have afforded a family of yellow complexes [42] (**1-R**, Chart 1) in decent yields. Preliminary (microanalytical and spectroscopic) characterizations on these complexes, although gave some idea about their composition, failed to indicate any definite formulation for them. For an unambiguous identification of these complexes, structure of a selected member of the family, *viz.* **1-CH$_3$**, has been determined by X-ray crystallography. The structure is shown in Fig. 1 and selected bond parameters are listed in Table 1. The structure reveals that two 1,3-diaryltriazenes are coordinated to rhodium, via loss of the N–H proton, in the monoanionic bidentate N,N-fashion forming four-membered chelate rings (**I**). A 4-methylphenyl fragment, probably generated *in situ* via cleavage of a C–N bond of the triazene ligand, is also found to be coordinated to the metal center in an η^1-fashion. The sixth coordination site on the metal center has been occupied by a triphenylphosphine. The coordinated 4-methylphenyl fragment and the triphenylphosphine are mutually cis. In this complex rhodium is therefore sitting in a CN_4P coordination environment, which is distorted significantly from ideal octahedral geometry, as reflected in the bond parameters around rhodium. This distortion is particularly attributable to the strain imposed by formation of the four-membered chelate rings with relatively small bite angles (61.5(4)° and 58.8(3)°) by the triazene ligands. The Rh–P and Rh–C distances are all quite normal, and so are the Rh–N distances [2–5,9,12], except the Rh(1)–N(1B) distance, which is slightly longer than usual. The observed elongation of the Rh(1)–N(1B) bond, which is trans to the Rh(1)–C(1C) bond, may be due to the trans effect of the coordinated 4-methylphenyl fragment [43–45]. The bond lengths within the coordinated triazene ligands are also quite usual [14–24]. Absence of any solvent of crystallization in the lattice of **1-CH$_3$** indicates possible existence of non-covalent interaction(s) between the individual complex molecules. A closer look at the packing pattern of the crystal reveals that η^1 and η^2 C–H···π interactions, involving both phenyl and methyl C–H, are active in the lattice (Fig. S1). Each

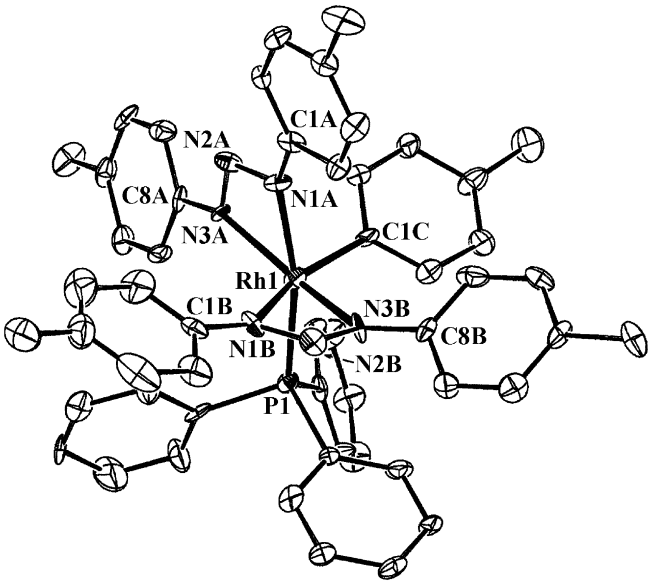

Fig. 1. View of the **1-CH$_3$** complex.

complex molecule is thus linked with the surrounding complex molecules through such C–H···π interactions, and these extended intermolecular interactions seem to hold the crystal together. It may be relevant to note here that such non-covalent interactions are of significant importance in crystal engineering and biology [46–57]. As all the **1-R** complexes (Chart 1) have been synthesized similarly and they show similar properties (*vide infra*), the other four **1-R** ($R \neq CH_3$) complexes are assumed to have similar structures as **1-CH$_3$**.

Formation of the η^1-bound aryl complexes of rhodium (**1-R**) via C–N bond cleavage of the 1,3-diaryltriazenes has been quite interesting. Examples of such η^1-bound aryl complexes are relatively less common in the literature [58–73]. It may be added in this context that metal mediated C–N bond cleavage, though not very uncommon, is mostly limited to strained amines and amidines [74–79], and hence there is significant interest in transition metal mediated C–N bond cleavage [80–89]. While the exact mechanism behind the observed C–N bond cleavage during formation of the **1-R** complexes is not completely clear to us, some speculated sequences, that seem probable, are illustrated in Scheme 1. In the initial step a 1,3-diaryltriazene reacts with the metal center in

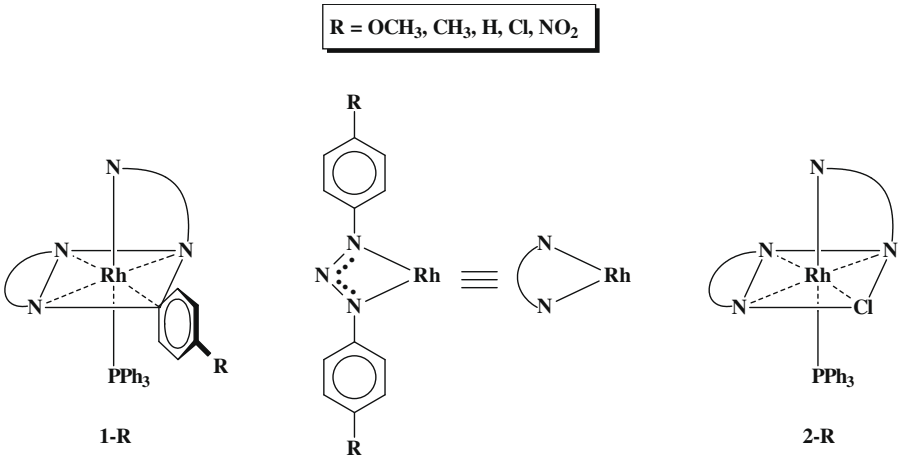

Chart 1.

Table 1
Selected bond lengths (Å) and bond angles (°) for the **1-CH$_3$** and **2-CH$_3$** complexes.

1-CH$_3$			
Bond lengths (Å)			
Rh(1)–C(1C)	2.034(9)	C(1)A–N(1A)	1.397(13)
Rh(1)–N(1A)	2.087(9)	N(1A)–N(2A)	1.357(16)
Rh(1)–N(3A)	2.079(9)	N(2A)–N3(A)	1.303(15)
Rh(1)–N(1B)	2.194(7)	N(3A)–C(8A)	1.424(14)
Rh(1)–N(3B)	2.080(9)	C(1B)–N(1B)	1.421(10)
Rh(1)–P(1)	2.312(3)	N(1B)–N(2B)	1.317(14)
		N(2B)–N(3B)	1.312(12)
		N(3B)–C(8B)	1.396(12)
Bond angles (°)			
P(1)–Rh(1)–N(1A)	166.5(3)	N(1A)–Rh(1)–N(3A)	61.5(4)
N(3A)–Rh(1)–N(3B)	160.6(4)	N(1B)–Rh(1)–N(3B)	58.8(3)
N(1B)–Rh(1)–C(1C)	158.6(5)		
2–CH$_3$			
Bond lengths (Å)			
Rh(1)–N(1)	2.083(7)	C(1)–N(1)	1.385(10)
Rh(1)–N(3)	2.050(8)	N(1)–N(2)	1.277(11)
Rh(1)–N(4)	2.058(6)	N(2)–N(3)	1.347(9)
Rh(1)–N(6)	2.072(9)	N(3)–C(8)	1.421(11)
Rh(1)–P(1)	2.326(2)	C(15)–N(4)	1.433(10)
Rh(1)–Cl(1)	2.332(3)	N(4)–N(5)	1.264(11)
		N(5)–N(6)	1.290(11)
		N(6)–C(22)	1.380(12)
Bond angles (°)			
P(1)–Rh(1)–N(6)	168.3(2)	N(1)–Rh(1)–N(3)	61.0(3)
N(1)–Rh(1)–N(4)	155.5(3)	N(4)–Rh(1)–N(6)	59.7(3)
N(3)–Rh(1)–Cl(1)	162.6(2)		

[Rh(PPh$_3$)$_3$Cl], whereby oxidative insertion of rhodium into the N–H bond takes place with simultaneous and usual dissociation of a PPh$_3$ from the metal center, affording a hydride intermediate. Subsequently the Rh–Cl bond is believed to transform into a Rh–H bond. Conversion of a M–Cl bond into a M–H bond in alcoholic medium in the presence of a base is well precedent in the literature [90–92]. This dihydride intermediate then reacts with a second triazene ligand, which links itself to the metal center as a N,N-donor, probably via initial acid–base reaction between the N–H proton of the triazene ligand and the metal-bound hydride leading to elimination of molecular hydrogen [93], followed by displacement of another PPh$_3$. A third triazene ligand is assumed to react next, whereby a hydride transfer to the triazene takes place leading to a N–N bond cleavage, producing aniline (or *para*-substituted aniline) and an anionic Ar–N$_2$ fragment that remains coordinated to the metal center as an N-donor. Generation of aniline (or *para*-substituted aniline) in the reaction vessel has been confirmed by gas chromatography. In the subsequent steps rearrangement from N-coordination to C-coordination of the anionic Ar–N$_2$ fragment occurs, followed by a C–N bond cleavage, leading to elimination of molecular nitrogen and formation of **1-R** [93]. It may be noted that yield of the **1-R** complexes is sensitive to the Rh:L ratio. The yield is optimum when the ratio is 1:3, and decreases when lesser amount of ligand is used. Though one triazene ligand can, in principle, provide two aryl fragments, the maximum yield of **1-R** with Rh:L ratio of 1:3 corroborates the proposition made in Scheme 1 that only one η^1-bound aryl fragment is provided by one triazene ligand. It may also be noted here that synthetic reactions carried out in the absence of the base (NEt$_3$) did not afford any **1-R** complex. This indirectly supports generation and involvement of the second hydride during the course of the synthetic reaction, which seems to play a key role in the observed N–N and C–N bond cleavage of the third triazene ligand.

In order to authenticate the role of solvent (ethanol) in converting a Rh–Cl bond into a Rh–H bond, and thereby promoting the observed C–N bond cleavage, similar reactions between [Rh(PPh$_3$)$_3$Cl] and the 1,3-diaryltriazenes were carried out in a non-alcoholic solvent, *viz*. toluene, which afforded a series of reddish-orange complexes (**2-R**, Chart 1). Preliminary characterizations hinted that, compared to the **1-R** complexes, these **2-R** complexes have different compositions. Identity of this new group of complexes was unveiled by structural characterization of a representative member, *viz*. **2-CH$_3$**, by X-ray crystallography. The structure (Fig. 2) shows that two triazene ligands are bound to rhodium as N,N-donors (**I**) and are mutually cis. A triphenylphosphine and a chloride are also coordinated to the metal center. The Rh–Cl distance is quite normal [2], and the other bond distances (Table 1) compare well with those observed in **1-CH$_3$**. It is to be noted here that in the absence of any coordinated 4-methylphenyl fragment (as in **1-CH$_3$**), the corresponding trans Rh–N(3) bond, which is now trans to the chloride, has not suffered any elongation. To find out the nature of intermolecular interactions in the lattice of **2-CH$_3$** its packing pattern has been examined, which shows that both C–H···N and η^1 C–H···π interactions are active (Fig. S2) and they link the individual complex molecules to form a stable lattice. In view of the similarity of their synthesis and properties, the other four **2-R** (R ≠ CH$_3$) complexes are believed to have similar structures as **2-CH$_3$**. It is relevant to mention here that a report incorporating synthesis of three **2-R** complexes (R = H, CH$_3$, and Cl) exists in the literature [94].

The observation that no C–N bond cleavage of the triazene ligand took place in toluene shows the influence of solvent variation on the nature of product obtained. It is also to be noted that variation of Rh:L ratio from 1:2 to 1:3 does not have any influence on the nature or yield of the product. The speculated sequences behind formation of the **2-R** complexes are shown in Scheme 2. The sequences are similar to the initial two steps in Scheme 1, except the Rh–Cl bond remains intact in toluene. It appears that inability of the Rh–Cl bond to transform into a Rh–H bond in toluene has contributed to all the observed differences. Attempts to convert **2-R** complexes into the corresponding **1-R** complexes have been made by reacting **2-R** with another mole of the respective 1,3-diaryltriazene in ethanolic medium in the presence of NEt$_3$. However, such reactions never gave the targeted **1-R** complexes, instead tris-triazenide complexes of rhodium were obtained in very low yields [95]. This shows that reactivity of the Rh–H fragment in the active bis-triazenide intermediate in Scheme 1 towards the third triazene ligand is different than that of the Rh–Cl fragment in the **2-R** complex.

2.2. Spectral studies

Infrared spectra of the **1-R** and **2-R** complexes show many bands of varying intensities within 4000–400 cm^{-1}. Assignment of each individual band to a specific vibration has not been attempted. However, the N–H stretches observed in the spectra of the uncoordinated triazene ligands around 3205 cm^{-1} are found to be absent in the spectra of the complexes, supporting loss of this N–H proton upon complexation. The ν(NN) bands arising from the triazene fragment appear around 1284 and 1500 cm^{-1} for all the complexes [21]. Three strong bands, observed near 526, 690 and 754 cm^{-1} in the **1-R** and **2-R** complexes, are attributable to the coordinated triphenylphosphines.

All the **1-R** and **2-R** complexes are diamagnetic, which corresponds to the trivalent state of rhodium (low-spin d^6, $S = 0$) in them. ^{1}H NMR spectra of these complexes have been recorded in CDCl$_3$ solution. In the spectra of the **1-R** complexes, signals for the coordinated triphenylphosphines are observed as broad peaks within 6.9–7.5 ppm. Some of the aromatic proton signals from the coordinated triazene ligands, as well as from the metal-bound phenyl fragment, could be clearly identified, while others could not be detected due to overlap problem. In the **1-CH$_3$** and **1-OCH$_3$** complexes, five distinct signals were observed for the methyl and

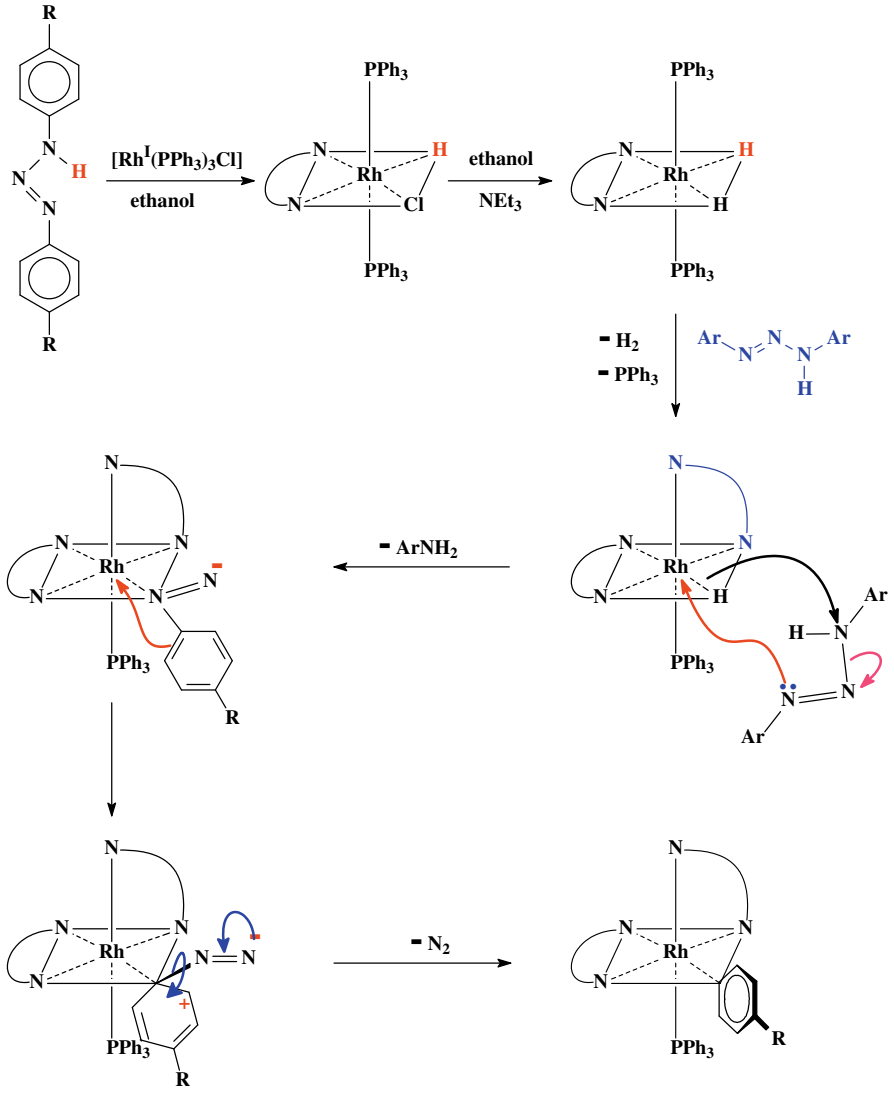

Scheme 1. Probable steps of the formation of the **1-R** complexes.

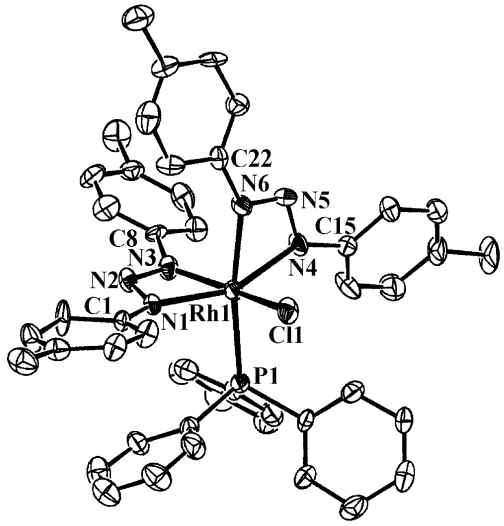

Fig. 2. View of the **2-CH$_3$** complex.

methoxy substituents, respectively. The ^{1}H NMR spectral features of the **2-R** complexes are qualitatively similar to those of the corresponding **1-R** complexes except that the triphenylphosphine signals could not be detected due to overlap problem. The non-equivalent nature of the two coordinated triazene ligands, as observed in the ^{1}H NMR spectra of the **1-R** and **2-R** complexes, is consistent with their representative crystal structures.

Electronic spectra of all the complexes have been recorded in dichloromethane solution. Spectral data are presented in Table 2. Spectrum of a selected **1-R** complex is shown in Fig. 3 and that of a representative **2-R** complex are deposited as Supplementary material (Fig. S3). Each complex shows several intense absorptions in the visible and ultraviolet region. The absorptions in the ultraviolet region are believed to be due to transitions within the ligand orbitals. To have an insight into the nature of absorptions in the visible region, semi-empirical EHMO calculations [96] have been performed on computer-generated models of all the complexes [97]. The results are found to be qualitatively similar for all the complexes [98]. Compositions of some selected molecular orbitals are given in Table S1 and partial MO diagram of a representative **1-R** complex is shown in Fig. 4. Partial MO diagram of selected **2-R** complex is deposited as Supplementary material (Fig. S4). The calculations show that in the **1-R** complexes the highest occupied molecular orbital (HOMO) has major (>50%) contribution from

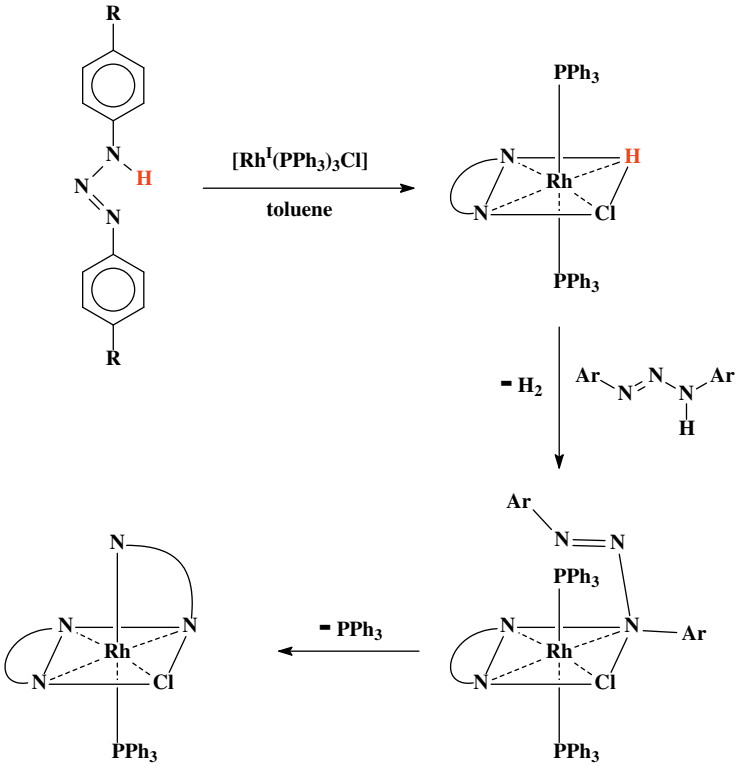

Scheme 2. Probable steps of the formation of the **2-R** complexes.

Table 2
Electronic spectral and cyclic voltammetric data for the **1-R** and **2-R** complexes.

Compounds	Electronic spectral data[a] λ_{max}, nm (ε, M^{-1} cm^{-1})	Cyclic voltammetric data[b] E, V vs. SCE	
		Oxidative responses	Reductive response
1-OCH$_3$	245 (45600), 406 (27200)	0.76,[d] 1.22[d]	−1.06[g]
1-CH$_3$	243 (47600), 403 (22800)	0.92,[d] 1.20[d]	−1.23[g]
1-H	244 (45800), 398 (20300)	1.08,[d] 1.31[d]	−1.08[g]
1-Cl	245 (48400), 399 (26100)	1.15,[d] 1.36[d]	−1.03[g]
1-NO$_2$	225[c] (37200), 299[c] (11900), 481 (17000)	1.68[d]	−1.01[g]
2-OCH$_3$	259[c](45700), 303[c] (35200), 408 (32600)	1.02[e](70),[f] 1.26[d]	−1.25 [g]
2-CH$_3$	252[c] (38700), 287[c] (26600), 401 (24700)	1.05[e](70),[f] 1.35[d]	−1.19 [g]
2-H	252[c] (46400), 282[c] (29200), 397 (24400)	1.17[e](70),[f] 1.42[d]	−1.19 [g]
2-Cl	255[c] (42000), 287[c] (36100), 401 (34100)	1.29[e](80),[f] 1.31[d]	−1.18 [g]
2-NO$_2$	267[c] (17700), 332 (13600), 454 (15700)	1.53[e](80)[f]	−0.96 [g]

[a] In dichloromethane solution.
[b] Solvent: 1:9 dichloromethane–acetonitrile; supporting electrolyte: TBAP; scan rate: 50 mV s^{-1}.
[c] Shoulder.
[d] E_{pa} value, where E_{pa} is the anodic peak potential.
[e] $E_{1/2} = 0.5(E_{pa} + E_{pc})$, where E_{pc} is the cathodic peak potential.
[f] $\Delta E_p = (E_{pa} - E_{pc})$.
[g] E_{pc} value.

the metal d-orbitals. The next two filled molecular orbitals (HOMO − 1 and HOMO − 2) also have significant contribution from rhodium. The lowest unoccupied molecular orbital (LUMO) is localized almost entirely on one 1,3-diaryltriazenide ligand and is concentrated mostly (>50%) on the triazene fragment [98]. The next vacant molecular orbital (LUMO + 1), which is relatively closer to the LUMO, is localized on the second 1,3-diaryltriazene ligand. Hence the lowest energy absorption near 400 nm may be assigned to an electronic transition from the filled rhodium orbital (HOMO) to the vacant π^*-orbital (LUMO) localized on the triazene fragment of a coordinated 1,3-diaryltriazene ligand. Composition of the frontier orbitals in the **2-R** complexes is qualitatively similar in nature to those in the corresponding **1-R** complexes, and hence in these complexes the lowest energy absorption in the visible region is assignable to a transition from filled rhodium orbital (HOMO) to vacant π^*-triazene orbital (LUMO). The relatively high intensities of the charge-transfer transitions in the visible region tempted us to explore the luminescence properties of these complexes. In ethanol solution at ambient temperature (298 K) all the complexes have been found to display emission in the visible region using an excitation wavelength of ~400 nm [99] (Fig. 3, Fig. S3). Quantum yields (ϕ) of these emissions have been evaluated (Table 3) with reference to $[Ru(bpy)_3]Cl_2$ (ϕ = 0.028 at 298 K) [100,101]. It may be mentioned here that electronic spectra of the **1-R** and

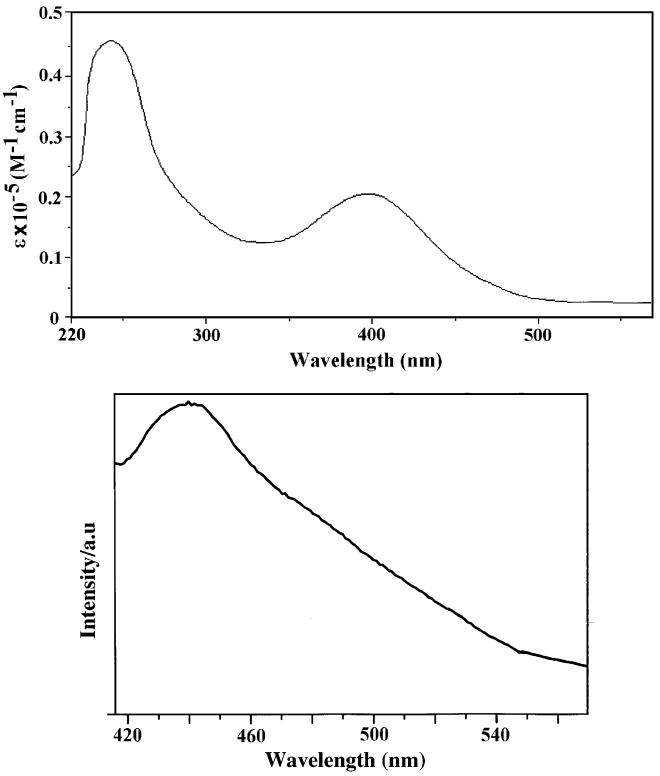

Fig. 3. Electronic spectrum (top) and emission spectrum (bottom) of the **1-H** complex.

2-R complexes have also been recorded in ethanol and they show identical characteristics to those recorded in dichloromethane solution.

2.3. Electrochemical properties

Electrochemical properties of the **1-R** and **2-R** complexes have been studied by cyclic voltammetry in 1:9 dichloromethane–acetonitrile solution (0.1 M TBAP) [102]. Voltammetric data are presented in Table 2 and representative voltammograms for **1-R** and **2-R** complexes are deposited as Supplementary material (Fig. S5 and S6). All the complexes show two oxidative responses on the positive side of SCE [103] and a reductive response on the negative side. In view of the composition of the HOMO (*vide infra*) the first oxidation is assigned to Rh(III)–Rh(IV) oxidation. The second oxidation is tentatively attributed to the oxidation of a coordinated triazene ligand. In the **1-R** complexes, both the oxidative responses are irreversible in nature. However, in the **2-R** complexes the first oxidative response is reversible in nature, characterized by a peak-to-peak separation (ΔE_p) of 70–80 mV, which remains unchanged upon changing the scan rate, and the anodic peak-current (i_{pa}) is almost equal to the cathodic peak-current (i_{pc}). The second oxidation is again irreversible in the **2-R** complexes. The reductive response is irreversible for all the complexes and, based on the composition of the LUMO, is assigned to reduction of the triazene fragment in the coordinated ligand. Potential of the Rh(III)–Rh(IV) oxidation in the **1-R** complexes is found to be sensitive to the nature of the substituent R in the coordinated ligand. The potential increases with increasing electron-withdrawing character of the substituent *R*. The plot of E_{pa} vs. 5σ [104] [σ = Hammett constant of *R* [105], $OCH_3 = -0.27$, $CH_3 = -0.17$, H = 0.00, Cl = 0.23 and $NO_2 = 0.78$] is linear (Fig. S7) with a slope (ρ) of 0.17 V (ρ = reaction constant of this couple [106]). A similar linear plot of Rh(III)–Rh(IV) oxidation potential vs. 4σ, with a slope (ρ) of 0.12 V is also observed for the **2-R** complexes (Fig. S8). The observed linear correlations in the **1-R** and **2-R** complexes show that the substituents (*R*) on the coordinated 1,3-diaryltriazene ligands, which are six-bonds away from the metal center [104], can still influence the metal-centered oxidation potential in a predictable manner.

3. Conclusions

The present study shows that the 1,3-diaryltriazenes (**L**) can readily undergo N–H bond activation upon reaction with $[Rh(PPh_3)_3Cl]$, and, depending on the nature of the reaction medium, they can also undergo N–N and C–N bond cleavage to afford η^1-bonded aryl complexes. The present exercise also shows that organic molecules that can potentially serve as bidentate ligands via loss of an acidic proton may also undergo similar activation reactions, and such possibilities are currently under investigation.

4. Experimental

Commercial rhodium trichloride was purchased from Arora Matthey, Kolkata, India. The *para*-substituted anilines were obtained from S.D., India. All other chemicals and solvents were reagent grade commercial materials and were used as received. $[Rh(PPh_3)_3Cl]$ was prepared following a reported procedure [107]. The 1,3-diaryltriazenes (**L**) were prepared by following a literature method [108]. Purification of acetonitrile and dichloromethane, and preparation of tetrabutylammonium perchlorate (TBAP) for electrochemical work were performed as reported in the literature [109,110]. Microanalyses (C, H, N) were performed using a Heraeus Carlo Erba 1108 elemental analyzer. The gas chromatographic measurements were done in a VARIAN CP-3800 gas chromatograph equipped with an FID detector. A CP-Sil 8 CB capillary column was used for analysis of the product. ^{1}H NMR spectra were recorded in $CDCl_3$ solution on a Bruker Avance DPX 300 NMR spectrometer using TMS as the internal standard. IR spectra were obtained on a Shimadzu FTIR-8300 spectrometer with samples prepared as KBr pellets. Electronic spectra were recorded on a JASCO V-570 spectrophotometer. Emission spectra were recorded in a Jobin Yvon Horiba FluoroMax 3 Luminescence Spectrometer. Electrochemical measurements were made using a CH Instruments model 600A electrochemical analyzer. A platinum disc working electrode, a platinum wire auxiliary electrode and an aqueous saturated calomel reference electrode (SCE) were used in the cyclic voltammetry experiments. All electrochemical experiments were performed under a dinitrogen atmosphere. All electrochemical data were collected at 298 K and are uncorrected for junction potentials.

4.1. Synthesis of complexes

1-R: The **1-R** complexes were synthesized by following a general procedure. Specific details are given below for a particular complex.

1-OCH_3: 1,3-Di(4′-methoxyphenyl)triazene (85 mg, 0.33 mmol) was dissolved in ethanol (40 mL) and triethylamine (35 mg, 0.35 mmol) was added to it [41]. The solution was then purged with a stream of dinitrogen for 10 min and to it was added $[Rh(PPh_3)_3Cl]$ (100 mg, 0.11 mmol). The resulting mixture was then heated to reflux under a dinitrogen atmosphere for 6 h to yield a yellow solution. The solution was evaporated and the solid residue, thus obtained, was purified by thin layer chromatography on a silica plate. Using 1:1 hexane–benzene as the eluant, a yellow band separated, which was extracted with acetonitrile. On evaporation of

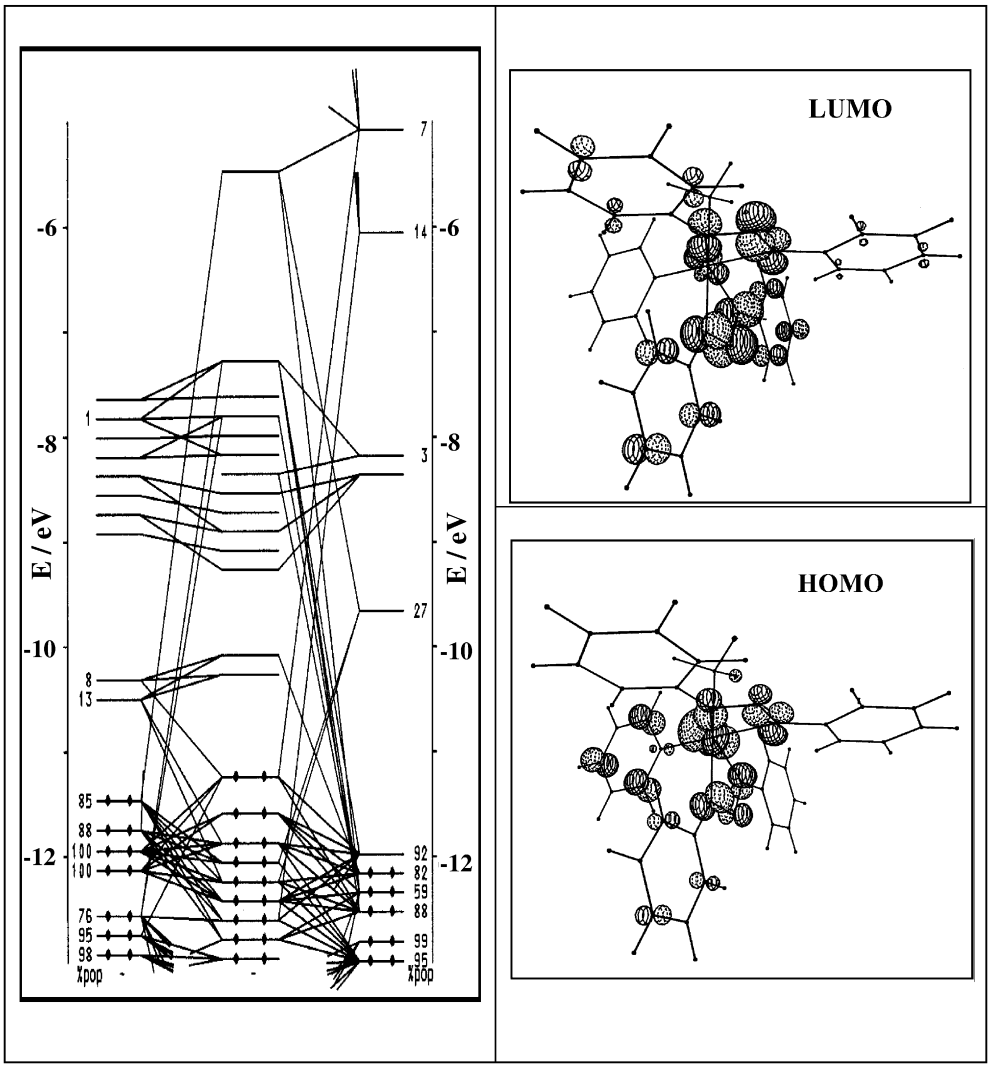

Fig. 4. Partial molecular orbital diagram of the **1-H** complex.

the acetonitrile extract, complex **1-OCH$_3$** was obtained as a crystalline yellow solid. Yield: 60%. Anal. Calc. for $C_{53}H_{50}O_5N_6PRh$: C, 64.64; H, 5.08; N, 8.54. Found: C, 64.61; H, 5.06; N, 8.56%. ^{1}H NMR [111]: 3.64 (OCH_3); 3.67 (OCH_3); 3.69 (OCH_3); 3.78 (OCH_3); 3.81 (OCH_3); 6.42 (d, 2H, J = 8.6); 6.59 (4H)*; 6.73 – 6.84 (12H)*; 6.91 (d, 2H, J = 8.1); 7.00–7.16 (PPh_3).

Table 3
Emission spectral data for the **1-R** and **2-R** complexes.

Compounds	Emission data		
	λ_{max} (nm)		Quantum yield (ϕ)
	Excitation	Emission	
1-OCH$_3$	406	431	0.012
1-CH$_3$	403	430	0.012
1-H	398	440	0.015
1-Cl	399	426	0.029
1-NO$_2$	481	554	0.010
2-OCH$_3$	408	451	0.015
2-CH$_3$	401	470	0.006
2-H	397	445	0.014
2-Cl	401	445	0.014
2-NO$_2$	454	531	0.026

1-CH$_3$: Yield: 70%. Anal. Calc. for $C_{53}H_{50}N_6PRh$: C, 70.36; H, 5.53; N, 9.29. Found: C, 70.36; H, 5.50; N, 9.31%. ^{1}H NMR: 2.13 (CH_3); 2.17 (CH_3); 2.22 (CH_3); 2.27 (CH_3); 2.28 (CH_3); 6.56 (d, 2H, J = 7.7); 6.67 (d, 2H, J = 8.2); 6.75 (d, 2H, J = 7.9); 6.79–6.86 (8H)*; 6.91 (d, 2H, J = 7.7); 6.99–7.18 (PPh_3); 7.21–7.26 (4H)*.

1-H: Yield: 62%. Anal. Calc. for $C_{48}H_{40}N_6PRh$: C, 69.07; H, 4.80; N, 10.08. Found: C, 69.03; H, 4.77; N, 10.11%. ^{1}H NMR: 6.74 (4H)*; 6.90–6.95 (6H)*; 7.03-7.22 (30H)*.

1-Cl: Yield: 65%. Anal. Calc. for $C_{48}H_{35}N_6PCl_5Rh$: C, 57.23; H, 3.48; N, 8.35. Found: C, 57.19; H, 3.47; N, 8.37%. ^{1}H NMR: 6.70–6.76 (8H)*; 6.80 (d, 2H, J = 6.8); 6.86 (d, 2H, J = 8.9); 7.02 (d, 2H, J = 8.4); 7.05–7.16 (PPh_3); 7.20 (d, 2H, J = 8.8); 7.31–7.34 (4H)*.

1-NO$_2$: Yield: 58%. Anal. Calc. for $C_{48}H_{35}N_{11}O_{10}PRh$: C, 54.40; H, 3.31; N, 14.54. Found: C, 54.36; H, 3.31; N, 14.60%. ^{1}H NMR: 6.87 (4H)*; 7.05 (d, 2H, J = 7.0); 7.18 (4H)*; 7.35–7.48 (PPh_3); 7.52–7.61 (6H)*; 7.66 (4H)*.

2-R: The **2-R** complexes were synthesized by following a general procedure. Specific details are given below for a particular complex.

2-OCH$_3$: 1,3-Di(4′-methoxyphenyl)triazene (60 mg, 0.23 mmol) was dissolved in toluene (40 mL) and triethylamine (25 mg, 0.25 mmol) was added to it [112]. The solution was then purged with a stream of dinitrogen for 10 min and [$Rh(PPh_3)_3Cl$] (100 mg, 0.11 mmol) was added to it. The resulting mixture was

Table 4
Crystallographic data for the **1-CH$_3$** and **2-CH$_3$** complexes.

	1-CH$_3$	**2-CH$_3$**
Empirical formula	$(C_{53}H_{50}N_6PRh)_2$	$(C_{46}H_{43}ClN_6PRh)_2$
Fw	1809.74	1698.38
Space group	Monoclinic, $P2_1/c$	Triclinic, $P\bar{1}$
Unit cell dimensions		
a (Å)	22.6313(14)	10.5012(15)
b (Å)	17.4488(6)	14.372(2)
c (Å)	25.3688(12)	14.761(2)
α (°)	90	102.378(2)
β (°)	115.237(6)	106.372(2)
γ (°)	90	90.093(2)
V (Å ^{3})	9061.7(9)	2083.2(5)
Z	8	2
λ (Å)	0.71073	0.71073
Crystal size (mm)	0.19 × 0.37 × 0.41	0.05 × 0.05 × 0.05
T (K)	203	295
μ (mm^{-1})	0.455	0.552
R_1[a]	0.1827	0.0369
wR_2[b]	0.5007	0.1101
GOF[c]	1.14	0.82

[a] $R_1 = \sum||F_o| - |F_c||/\sum|F_o|$.
[b] $wR_2 = [\sum\{w(F_o^2 - F_c^2)^2\}/\sum\{w(F_o^2)\}]^{1/2}$.
[c] GOF = $[\sum(w(F_o^2 - F_c^2)^2)/(M - N)]^{1/2}$, where *M* is the number of reflections and *N* is the number of parameters refined.

then heated to reflux under a dinitrogen atmosphere for 24 h, whereby an orangish-yellow solution was produced. Evaporation of this solution gave an orange solid, which was subjected to purification by thin layer chromatography on a silica plate. Using 1:1 hexane–benzene as the eluant a reddish-orange band separated, which was extracted with acetonitrile. On evaporation of the acetonitrile extract complex **2-OCH$_3$** was obtained as a reddish-orange crystalline solid. Yield: 65%. Anal. Calc. for $C_{46}H_{43}N_6O_4PClRh$: C, 60.50; H, 4.71; N, 9.21. Found: C, 60.59; H, 4.70; N, 9.18%. ^{1}H NMR: 3.69 (OCH_3); 3.73 (OCH_3); 3.76 (OCH_3); 3.80 (OCH_3); 6.50 (d, 2H, *J* = 8.6); 6.64 (4H)*; 6.85 (d, 2H, *J* = 9.0); 6.93–7.04 (10H)*; 7.23–7.28 (9H)*; 7.46 (4H)*.

2-CH$_3$: Yield: 63%. Anal. Calc. for $C_{46}H_{43}N_6PClRh$: C, 65.06; H, 5.07; N, 9.90. Found: C, 65.10; H, 5.04; N, 9.89%. ^{1}H NMR: 2.20 (CH_3); 2.24 ($2CH_3$)*; 2.31 (CH_3); 6.74 (d, 2H, *J* = 8.1); 6.81–7.02 (18H)*; 7.22–7.25 (7H)*; 7.46 (4H)*.

2-H: Yield: 60%. Anal. Calc. for $C_{42}H_{35}N_6PClRh$: C, 63.60; H, 4.42; N, 10.60. Found: C, 63.62; H, 4.42; N, 10.59%. ^{1}H NMR: 6.98–7.24 (31H)*; 7.37 (t, 2H, *J* = 9.2); 7.49 (t, 2H, *J* = 9.5).

2-Cl: Yield: 65%. Anal. Calc. for $C_{42}H_{31}N_6PCl_5Rh$: C, 54.17; H, 3.33; N, 9.03. Found: C, 54.20; H, 3.33; N, 9.01%. ^{1}H NMR: 6.82 (d, 2H, *J* = 8.5); 6.92 (d, 4H)*; 7.04–7.12 (12H)*; 7.18 (d, 2H, *J* = 8.9); 7.26–7.35 (7H)*; 7.46 (4H)*.

2-NO$_2$: Yield: 62%. Anal. Calc. for $C_{42}H_{35}O_8N_{10}PClRh$: C, 51.83; H, 3.19; N, 14.40. Found: C, 51.87; H, 3.14; N, 14.37%. ^{1}H NMR: 6.84 (d, 2H, *J* = 8.6); 7.06–7.11 (4H)*; 7.16–7.23 (2d, 4H)*; 7.45 (d, 2H, *J* = 9.0); 7.64 (d, 2H, *J* = 8.0); 7.68–7.76 (13H)*; 7.97 (d, 2H, *J* = 9.0); 8.23 (d, 2H, *J* = 9.0).

4.2. X-ray structure determination

Single crystals of the **1-CH$_3$** and **2-CH$_3$** complexes were obtained by slow evaporation of acetonitrile solution of the complexes. Selected crystal data and data collection parameters are given in Table 4. Data were collected, respectively, on an Oxford Diffraction Gemini, a Bruker SMART Apex CCD area detector systems using graphite monochromated Mo Kα radiation (λ = 0.71073 Å). X-ray data reduction, structure solution and refinement were done using SHELXS-97 and SHELXL-97 programs [113]. The structures were solved by the direct methods.

Acknowledgments

The authors thank the reviewers for their constructive comments, which have been helpful in preparing the revised manuscript. Financial assistance received from the UGC-CAS program in the Department of Chemistry, Jadavpur University, is gratefully acknowledged. The authors thank the School of Chemistry, University of Hyderabad, for collecting data on the **2-CH$_3$** crystal, and also Dr. Subratanath Koner and Shreyashi Jana, Department of Chemistry, Jadavpur University, for gas chromatographic measurements. Chhandasi GuhaRoy thanks the University Grants Commission, New Delhi, for her fellowship [Grant No. 10-2(5)/2005(I)-E.U.II].

Appendix A. Supplementary material

CCDC 695864 and 695865 contain the supplementary crystallographic data for this paper. These data can be obtained free of charge from The Cambridge Crystallographic Data Centre via www.ccdc.cam.ac.uk/data_request/cif. Hydrogen-bonding interactions in complex **1-CH$_3$** (Fig. S1) and complex **2-CH$_3$** (Fig. S2), absorption and emission spectra of complex **2-H** (Fig. S3), partial MO diagrams of complex **2-H** (Fig. S4), cyclic voltammograms of complexes **1-CH$_3$** (Fig. S5) and complex **2-CH$_3$** (Fig. S6), Hammett plots for the **1-R** complexes (Fig. S7) and **2-R** complexes (Fig. S8), and compositions of selected molecular orbitals for the **1-R** and **2-R** complexes (Table S1) are available as supplementary material. Supplementary data associated with this article can be found, in the online version, at doi:10.1016/j.jorganchem.2008.10.006.

References

[1] F.H. Jardine, Prog. Inorg. Chem. 28 (1981) 63.
[2] S. Baksi, R. Acharyya, F. Basuli, S.M. Peng, G.H. Lee, M. Nethaji, S. Bhattacharya, Organometallics 26 (2007) 6596.
[3] S. Baksi, R. Acharyya, S. Dutta, A.J. Blake, M.G.B. Drew, S. Bhattacharya, J. Organomet. Chem. 692 (2007) 1025.
[4] S. Basu, S. Dutta, M.G.B. Drew, S. Bhattacharya, J. Organomet. Chem. 691 (2006) 3581.
[5] R. Acharyya, S. Dutta, F. Basuli, S.M. Peng, G.H. Lee, L.R. Falvello, S. Bhattacharya, Inorg. Chem. 45 (2006) 1252.
[6] S. Basu, I. Pal, R.J. Butcher, G. Rosair, S. Bhattacharya, J. Chem. Sci. 117 (2005) 167.
[7] S. Basu, S.M. Peng, G.H. Lee, S. Bhattacharya, Polyhedron 24 (2005) 157.
[8] R. Acharyya, F. Basuli, G. Rosair, S. Bhattacharya, New J. Chem. 28 (2004) 115.
[9] I. Pal, S. Dutta, F. Basuli, S. Goverdhan, S.M. Peng, G.H. Lee, S. Bhattacharya, Inorg. Chem. 42 (2003) 4338.
[10] S. Dutta, F. Basuli, S.M. Peng, G.H. Lee, S. Bhattacharya, New J. Chem. 26 (2002) 1607.
[11] A. Das, F. Basuli, S.M. Peng, S. Bhattacharya, Inorg. Chem. 41 (2002) 440.
[12] S. Dutta, S.M. Peng, S. Bhattacharya, J. Chem. Soc., Dalton Trans. (2000) 4623.
[13] S. Dutta, S.M. Peng, S. Bhattacharya, Inorg. Chem. 39 (2000) 2231.
[14] N. Nimitsiriwat, V.C. Gibson, E.L. Marshall, P. Takolpuckdee, A. K Tomov, A.J.P. White, D.J. Williams, M.R.J. Elsegood, S.H. Dale, Inorg. Chem. 46 (2007) 9988.
[15] G. Albertin, S. Antoniutti, M. Bedin, J. Castro, S. Garcia-Fontan, Inorg. Chem. 45 (2006) 3816.
[16] T. Clark, J. Cochrane, S.F. Colson, K.Z. Malik, S.T. Robinson, J.W. Steed, Polyhedron 20 (2001) 1875.
[17] D. Pfeiffer, I.A. Guzei, L.M. Liable-Sands, M.J. Heeg, A.L. Rheingold, C.H. Winter, J. Organomet. Chem. 588 (1999) 167.
[18] S. Westhusin, P. Gantzel, P.J. Walsh, Inorg. Chem. 37 (1998) 5956.
[19] M. Menon, A. Pramanik, S. Chattopadhyay, N. Bag, A. Chakravorty, Inorg. Chem. 34 (1995) 1361.
[20] J.T. Leman, J. Braddock-Wilking, A.J. Coolong, A.R. Barron, Inorg. Chem. 32 (1993) 4324.
[21] S.F. Colson, S.D. Robinson, Polyhedron 9 (1990) 1737.
[22] C. Carriedo, N.G. Connelly, R. Hettrich, A.G. Orpen, A.M.J. White, J. Chem. Soc., Dalton Trans. (1989) 745.
[23] G.L. Hillhouse, B.L. Haymore, Inorg. Chem. 26 (1987) 1876.
[24] M.A.M. Queiros, J.E.J. Simao, A.R. Dias, J. Organomet. Chem. 329 (1987) 85.
[25] C.J. Creswell, M.A.M. Queiros, S.D. Robinson, Inorg. Chim. Acta 60 (1982) 157.
[26] A. Immirzi, W. Porzio, G. Bombieri, L. Toniolo, J. Chem. Soc., Dalton Trans. (1980) 1098.
[27] L.D. Brown, J.A. Ibers, J. Am. Chem. Soc. 98 (1976) 1597.
[28] J.J. Nuricumbo-Escobar, C. Campos-Alvarado, G. Rios-Moreno, D. Morales-Morales, P.J. Walsh, M. Parra-Hake, Inorg. Chem. 46 (2007) 6182.

[29] C.J. Adams, R.A. Baber, N.O. Connelly, P. Hardeng, O.D. Hayward, M. Kandiah, A.G. Orpen, J. Chem. Soc., Dalton Trans. 13 (2007) 1325.
[30] C. Tejel, M.A. Ciriano, G. Rios-Moreno, I.T. Dobrinovitch, F.J. Lahoz, L.A. Oro, M. Parra-Hake, Inorg. Chem. 43 (2004) 4719.
[31] N.G. Connelly, O.D. Hayward, P. Klangsinsirikul, A.G. Orpen, J. Chem. Soc., Dalton Trans. (2002) 305.
[32] J. Ruiz, G.F.J. Lopez, V. Rodriguez, J. Perez, M.C. Ramirez de Arellano, G. Lopez, J. Chem. Soc., Dalton Trans. (2001) 2683.
[33] P. Gantzel, P.J. Walsh, Inorg. Chem. 37 (1998) 3450.
[34] H.G. Ang, L.L. Koh, G.Y. Yang, J. Chem. Soc., Dalton Trans. 8 (1996) 1573.
[35] N.G. Connelly, T. Einig, G. Garcia, G. Herbosa, P.M. Hopkins, C. Mealli, A.G. Orpen, G.M. Rosair, F. Viguri, J. Chem. Soc., Dalton Trans. (1994) 2025.
[36] M.B. Hursthouse, M.A. Mazid, T. Clark, D. Robinson, Polyhedron 12 (1993) 563.
[37] N.G. Connelly, G. Garcia, J. Chem. Soc., Dalton Trans. (1987) 2737.
[38] M.B.K. Smith, L.A. Taneyhill, C.J. Michejda, R.H. Smith Jr., Chem. Res. Toxicol. 9 (1996) 341.
[39] A.M. McConnaughie, T.C. Jenkins, J. Med. Chem. 38 (1995) 3488.
[40] R.H. Smith Jr., D.A. Scudiero, C.J. Michejda, J. Med. Chem. 33 (1990) 2579.
[41] The reaction does not occur in absence of base (NEt_3).
[42] The **1**-$\mathbf{NO_2}$ complex is yellowish orange.
[43] A. Cavaglioni, R. Cini, J. Chem. Soc., Dalton Trans. (1997) 1149.
[44] R. Cini, G. Giorgi, L. Pasquini, Inorg. Chim. Acta 196 (1992) 7.
[45] J.F. Hartwig, R.G. Bergman, R.A. Andersen, J. Am. Chem. Soc. 113 (1991) 3404.
[46] M.J. Calhorda, Chem. Commun. (2000) 801.
[47] C. Janiak, S. Temizdemir, S. Dechert, Inorg. Chem. Commun. 3 (2000) 271.
[48] C. Janiak, S. Temizdemir, S. Dechert, W. Deck, F. Girgsdies, J. Heinze, M.J. Kolm, T.G. Scarmann, O.M. Zipffel, Eur. J. Inorg. Chem. (2000) 1229.
[49] G.R. Desiraju, T. Steiner, The Weak hydrogen Bond (IUCr Monograph on Crystallography 9), Oxford Science Pub., 1999.
[50] M.J. Hannon, C.L. Painting, N.W. Alcock, Chem. Commun. (1999) 2023.
[51] B.J. Mcnelis, L.C. Nathan, C.J. Clark, J. Chem. Soc., Dalton Trans. (1999) 1831.
[52] K. Biradha, C. Seward, M.J. Zaworotko, Angew. Chem., Int. Ed. 38 (1999) 492.
[53] S.K. Burley, G.A. Petsko, Adv. Protein Chem. 39 (1998) 125.
[54] M. Nishio, M. Hirota, Y. Umezawa, The CH$\cdots\pi$ Interactions (Evidence, Nature and Consequences), Wiley-VCH, New York, 1998.
[55] Y. Umezawa, S. Tsuboyama, K. Honda, J. Uzawa, M. Nishio, Bull. Chem. Soc. Jpn. 71 (1998) 1207.
[56] N.N.L. Madhavi, A.K. Katz, H.L. Carrell, A. Nangia, G.R. Desiraju, Chem. Commun. (1997) 1953.
[57] H.C. Weiss, D. Blaser, R. Boese, B.M. Doughan, M.M. Haley, Chem. Commun. (1997) 1703.
[58] N.L. Kilah, S. Patrie, R. Stranger, J.W. Wielandt, A.C. Willis, S.B. Wild, Organometallics 26 (2007) 6106.
[59] A.H. Roy, C.P. Lenges, M. Brookhart, J. Am. Chem. Soc. 129 (2007) 2082.
[60] P. Zhao, C.D. Incarvito, J.F. Hartwig, J. Am. Chem. Soc. 129 (2007) 1876.
[61] V. Diez, G. Espino, F.A. Jalon, B.R. Manzano, M. Perez-Manrique, J. Organomet. Chem. 692 (2007) 1482.
[62] K. Mochida, T. Fukushima, M. Suzuki, W. Hatanaka, M. Takayama, Y. Usui, M. Nanjo, K. Akasaka, T. Kudo, S. Komiya, J. Organomet. Chem. 692 (2007) 395.
[63] S.J. Hoseini, M. Mohamadikish, K. Kamali, F.W. Heinemann, M. Rashidi, J. Chem. Soc., Dalton Trans. (2007) 1697.
[64] P. Nilson, G. Puxty, O.F. Wendt, Organometallics 25 (2006) 1285.
[65] J. Vicente, A. Arcas, M-D. Galvez-Lopez, P.G. Jones, Organometallics 25 (2006) 4247.
[66] C. Adamo, C. Amatore, I. Ciofini, A. Jutland, H. Lakmini, J. Am. Chem. Soc. 128 (2006) 6829.
[67] P. Zhao, C.D. Incarvito, J.F. Hartwig, J. Am. Chem. Soc. 128 (2006) 3124.
[68] A. Yahav, I. Goldberg, A. Vigalok, Inorg. Chem. 44 (2005) 1547.
[69] X. Wang, B.S. Lane, D. Sames, J. Am. Chem. Soc. 127 (2005) 4996.
[70] P. Zhao, J.F. Hartwig, J. Am. Chem. Soc. 127 (2005) 11618.
[71] J.A. Casares, P. Espinet, J.M. Martin-Alvarez, J.M. Martinez-Ilarduya, G. Salas, Eu. J. Inorg. Chem. (2005) 3825.
[72] F.L. Taw, A.H. Mueller, R.G. Bergman, M. Brookhart, J. Am. Chem. Soc. 125 (2003) 9808.
[73] F.L. Taw, P.S. White, R.G. Bergman, M. Brookhart, J. Am. Chem. Soc. 124 (2002) 4192.
[74] F.A. Cotton, L.M. Daniels, CA. Murillo, X. Wang, Inorg. Chem. 36 (1997) 896.
[75] F.A. Cotton, J.H. Matonic, C.A. Murillo, X. Wang, Bull. Soc. Chim. Fr. 133 (1996) 711.
[76] G. Proulx, R.G. Bergman, J. Am. Chem. Soc. 116 (1994) 7953.
[77] C.C. Cummins, R.R. Shrock, W.M. Davis, Inorg. Chem. 33 (1994) 1448.
[78] J.R. Agadorn, J. Arnold, Organometallics 13 (1994) 4670.
[79] L.M. Atagi, D.E. Over, D.R. McAlister, J.M. Mayer, J. Am. Chem. Soc. 113 (1991) 870.
[80] S. Ueno, N. Chatani, F. Kakiuchi, J. Am. Chem. Soc. 129 (2007) 6098.
[81] T. Saeki, E.-C. Son, K. Tamao, Org. Lett. 7 (2004) 617.
[82] O.V. Ozerov, C. Guo, V.A. Papkov, B.M. Foxman, J. Am. Chem. Soc. 126 (2004) 4792.
[83] C. Hu, R.M. Chin, T.D. Nguyen, K.T. Nguyen, P.S. Wagenknecht, Inorg. Chem. 42 (2003) 7602.
[84] T.M. Cameron, K.A. Abboud, M.J. Boncella, Chem. Commun. (2001) 1224.
[85] H. Werner, G. Horlin, W.D. Jones, J. Organomet. Chem. 562 (1998) 45.
[86] T.S. Kleckley, J.L. Bennett, P.T. Wolczanski, E.B. Lobkovsky, J. Am. Chem. Soc. 119 (1997) 247.
[87] M.-C. Rodriguez, F. Lambert, I. Morgenstern-Badarau, Inorg. Chem. 36 (1997) 3525.
[88] F.A. Cotton, L.M. Daniela, C.A. Murillo, X. Wang, Inorg. Chem. 36 (1997) 896.
[89] J.H. Hagadorn, J. Arnold, Organometallics 13 (1994) 4670.
[90] R. CelenligilCetin, L.A. Watson, C. Guo, B.M. Foxman, O.V. Ozerov, Organometallics 24 (2005) 186.
[91] T. Li, R. Churlaud, A.J. Lough, K. Abdur-Rashid, R.H. Morris, Organometallics 23 (2004) 6239.
[92] C.S. Yi, S.Y. Yun, I.A. Guzei, Organometallics 23 (2004) 5392.
[93] The evolved gas could not be detected.
[94] K.R. Laing, S.D. Robinson, M.F. Uttley, J. Chem. Soc., Dalton Trans. (1974) 1205.
[95] Identity of the tris-triazenide complexes was established by mass and ^{1}H NMR spectra [*e.g.*, for the tris-triazenide complex with R = CH_3, Yield: 2%. Mass: 776, $[M+H]^+$. ^{1}H NMR: 2.26 ($6CH_3$); 6.99 (d, 12H, J = 8.6); 7.16 (d, 12H, J = 8.1)].
[96] C. Mealli, D.M. Proserpio, J. Chem. Educ. 67 (1990) 399.
[97] In the **1**-**R** and **2**-**R** complexes the phenyl rings of the triphenylphosphines have been replaced by hydrogens.
[98] In the **1**-$\mathbf{NO_2}$ and **2**-$\mathbf{NO_2}$ complexes the LUMO has significant contributions from the NO_2 fragments.
[99] The excitation wavelength is different for the **1**-$\mathbf{NO_2}$ and **2**-$\mathbf{NO_2}$ complexes.
[100] M.J. Cook, A.P. Lewis, G.S.J. Thomson, J.L. Glasper, D.J. Robbins, J. Chem. Soc., Perkin Trans. (1984) 293.
[101] G.A. Crosby, W.H. Elfring Jr., J. Phys. Chem. 80 (1976) 2206.
[102] A little dichloromethane was necessary to take the complex into solution. Addition of large excess of acetonitrile was necessary to record the redox responses in proper shape.
[103] For the **1**-$\mathbf{NO_2}$ and **2**-$\mathbf{NO_2}$ complexes only one oxidation have been observed, probably because the other oxidation occurs beyond the voltage window.
[104] The substituent (R) on the η^1-bound aryl fragment was also assumed to have the same σ-value as the other four substituents on the two coordinated triazene ligands.
[105] L.P. Hammett, Physical Organic Chemistry, second ed., McGraw Hill, New York, 1970.
[106] R.N. Mukherjee, O.A. Rajan, A. Chakravorty, Inorg. Chem. 21 (1982) 785.
[107] J.A. Osborn, G. Wilkinson, Inorg. Synth. 10 (1967) 67.
[108] W.W. Hartman, J.B. Dickey, Org. Synth. 2 (1943) 163.
[109] D.T. Sawyer, J.L. Roberts Jr., Experimental Electrochemistry for Chemists, Wiley, New York, 1974. pp. 167–215.
[110] M. Walter, L. Ramaley, Anal. Chem. 45 (1973) 165.
[111] Chemical shifts are given in ppm and multiplicity of the signals along with the associated coupling constants (J in Hz) are given in parentheses. Overlapping signals are marked with an asterisk.
[112] The **2**-**R** complexes are also obtained in similar yield in the absence of any base.
[113] G.M. Sheldrick, SHELXS-97 and SHELXL-97, Fortran Programs for Crystal Structure Solution and Refinement, University of Gottingen, Gottingen, Germany, 1997.